



# IJRASET

International Journal For Research in  
Applied Science and Engineering Technology



---

# INTERNATIONAL JOURNAL FOR RESEARCH

IN APPLIED SCIENCE & ENGINEERING TECHNOLOGY

---

**Volume: 11    Issue: VIII    Month of publication: Aug 2023**

**DOI: <https://doi.org/10.22214/ijraset.2023.55353>**

**[www.ijraset.com](http://www.ijraset.com)**

**Call:  08813907089**

**E-mail ID: [ijraset@gmail.com](mailto:ijraset@gmail.com)**

# A Review of Numerical Simulation and Analytical Calculation Methods for the Study of Flow over a Wedge

Chintan R. Prajapati<sup>1</sup>, Aniket P. Donga<sup>2</sup>, Akshar D. Patel<sup>3</sup>, Pranav R. Babariya<sup>4</sup>

<sup>1, 2, 3, 4</sup>Department of Aeronautical Engineering, Silver Oak College of Engineering and Technology, Gujarat technological University, Ahmedabad

**Abstract:** *The study of flow over a wedge holds immense significance in diverse domains, encompassing aerodynamics and heat transfer applications. This research paper presents a comprehensive investigation of essential flow parameters, including pressure, temperature, velocity, and shock wave characteristics. Moreover, it offers a comparative analysis between analytical and numerical approaches for studying flow over a wedge.*

*Theoretical analyses involve calculating vital parameters like pressure ratio and temperature ratio using 1-D inviscid compressible flow equations coupled with conservation laws for energy, mass, and momentum. On the other hand, the numerical investigation employs Computational Fluid Dynamics (CFD) techniques, specifically the ANSYS Fluent CFD Code, to calculate a wide range of parameters and visualise the flow characteristics for the wedge geometry. In contrast, the ANSYS Fluent simulation employs 2-D inviscid compressible equations to conduct a detailed study of flow behaviour past the wedge geometry. Throughout the paper, the key flow parameters are meticulously analysed, taking into account both analytical and numerical results.*

*The comparisons between these two methodologies enable a comprehensive understanding of the advantages and limitations of each approach. Additionally, ANSYS Fluent CFD simulations facilitate the visualization of intricate flow patterns around the wedge, providing valuable insights into the fluid dynamics of the system.*

*This research paper contributes to the knowledge base by presenting a comprehensive review of numerical simulation and analytical calculation methods for the study of flow over a wedge. The insights gained from this analysis can aid researchers and engineers in selecting appropriate methodologies for specific flow scenarios, thus enhancing the efficiency and accuracy of future studies in this domain.*

**Keywords:** *Flow over a wedge, Fluid dynamics, Wedge, Shock wave, Numerical simulation, Analytical calculation, Computational Fluid Dynamics (CFD), Oblique shock wave relations, ANSYS Fluent CFD Code, Aerodynamics, Heat transfer.*

## I. NOMENCLATURE

- $\theta$  Wedge Deflection Angle
- $\beta$  Wave Angle
- M Mach Number
- p Pressure
- T Temperature
- $\gamma$  Specific heat ratio = 1.4 (for Air)
- $\mu$  Mach Angle

### Subscript

- 1 Before the Shock wave in the Region 1
- N1 Normal Component in the Region 1
- 2 After the Shock wave in the Region 2
- N2 Normal Component in the Region 2

## II. INTRODUCTION

A wedge is a geometric shape resembling a triangle with a sharp leading edge and a gradual or sharp trailing edge. It is widely studied to understand fluid flow around solid objects, particularly in high-speed or supersonic conditions. Figure 1 shows the wedge with a wedge angle  $15^\circ$ . Fig. 1 shows the wedge with a wedge angle  $15^\circ$ .

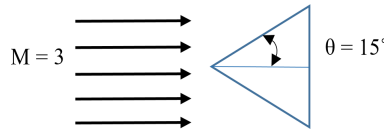


Fig.1 Geometry of the Wedge

When the high velocity passes over the shock that is created on the wedge, this shock can be an oblique shock or a Normal shock wave, and when the shock is an oblique shock, the region behind the shockwave is an extremely thin region, typically on the order of  $10^{-5}$  cm across which the flow properties can change drastically [1]. In the next section, some information is given about oblique shock waves.

### A. Oblique Shock Wave Relation: Analytical Solution

When flow passes the wedge, a weak shock is created over the surface of the wedge, which is inclined to the surface, and this shock is known as an oblique shock wave [2]. Below, Fig. 2 depicts the geometry of an oblique shock wave.

Now for the analytical solution, the oblique shock wave relations are:

As shown in Fig. 2, the free stream Mach number  $M_{N1}$  is normal to the shock wave, so for the calculation of the free stream Mach number, we used the normal shockwave relation because the component that is normal to the wedge is  $M_{N1}$  which is normal to the shock wave; hence, we used the normal shock wave relation with some algebraic form of the normal shock wave equation.

$$M_{N1} = M_1 \sin(\beta)$$

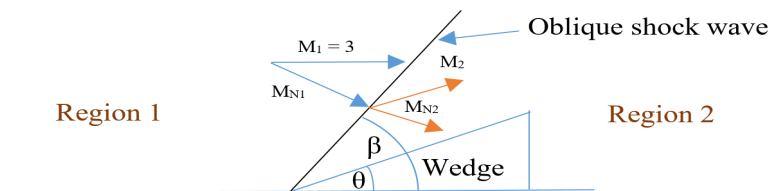


Fig. 2 Oblique shock wave geometry

From the above equation, we can find the Free stream Mach number; however, we need the wave angle  $\beta$  which can be taken from  $\theta$ - $\beta$ -M relation, which is shown in Fig. 3.

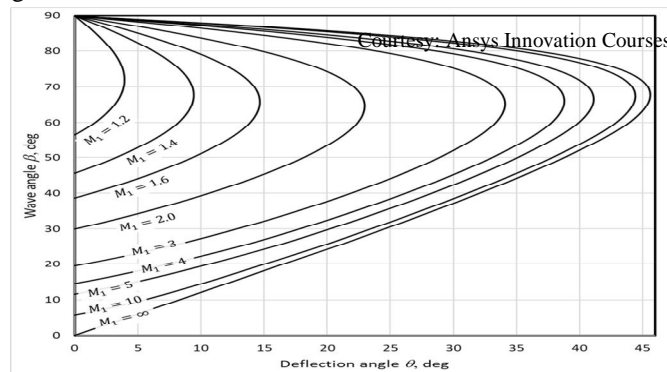


Fig. 3  $\theta$ - $\beta$ -M relation [17]

For the Deflection angle of  $15^\circ$  the corresponding wave angle at Mach 3 is around  $32.2404^\circ$  which is used in the theoretical solution for flow over a wedge.

Now we can enlist other relations for the calculation of the flow properties of an oblique shock wave using oblique shock wave relations.

$$M_{N2}^2 = \frac{1 + \left[\frac{\gamma - 1}{2}\right]M_{N1}^2}{\gamma M_{N1}^2 - \left[\frac{\gamma - 1}{2}\right]}$$

$$M_2 = \frac{M_{N2}}{\sin(\beta - \theta)}$$

$$\frac{p_2}{p_1} = 1 + \frac{2\gamma}{\gamma + 1} (M_{N1}^2 - 1)$$

$$\frac{T_2}{T_1} = \frac{(2\gamma M_{N1}^2 - (\gamma - 1))(\gamma - 1)M_{N1}^2 + 2}{(\gamma + 1)^2 M_{N1}^2}$$

Fig. 3 is the  $\theta$ - $\beta$ -M relation, which illustrates three physical phenomena associated with oblique shock waves.

For example: There is a maximum deflection angle  $\theta_{max}$  for each given upstream Mach number  $M_1$ . If the physical geometry is such that  $\theta > \theta_{max}$ , then no solution exists for a straight oblique shock wave. Instead, nature creates a curving shock wave that is not connected to a body's corner or nose (detached shock). This is depicted in Figure 4 [1].

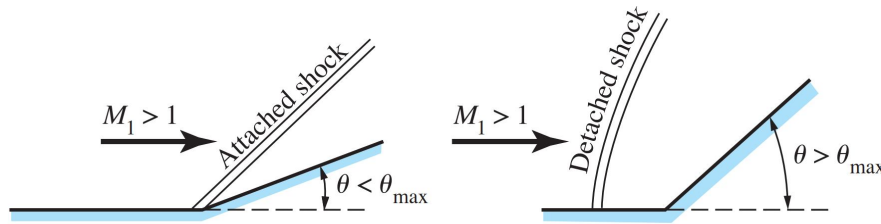


Fig. 4 Attached and detached shocks [1]

There are two straight oblique shock solutions for any given  $\theta$  less than  $\theta_{max}$  for any given upstream Mach number. For example, if  $M_1 = 3.0$  and  $\theta = 15^\circ$ , then from Figure 3,  $\beta$  can equal either  $32.24$  or  $85^\circ$ . The smaller value of  $\beta$  is called the weak shock solution, and the larger value of  $\beta$  is the strong shock solution. These two cases are illustrated in Fig. 5 [1].

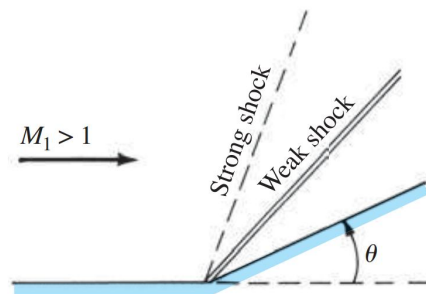


Fig. 5 The weak and strong shock cases [1]

If  $\theta = 0$ , then  $\beta$  equals either  $\mu$  or  $90^\circ$ . The case of  $\beta = 90^\circ$  corresponds to a normal shock wave [1].

### B. ANSYS Fluent: Numerical Simulation

Fluent is used in this current research to model the flow characteristics over the wedge. Fluent solves the three-dimensional Navier-Stokes equations by utilizing a finite element-based finite volume method over structured grids [3]. The CFD code is an integrated software system capable of solving diverse and complex multidimensional fluid flow problems. The fluid flow solver provides solutions for incompressible or compressible, steady-state or transient, laminar or turbulent single-phase fluid flow in complex geometries [4].



The grid generation procedure, which divides the computational domain into discrete sub-domains, is the first step in any numerical analysis. A grid must be provided in terms of the spatial coordinates of grid nodes distributed throughout the computational domain. The numerical analysis will establish values for all dependent variables, including pressure and velocity components, for each node in the domain. Creating the grid is the first step in calculating a flow Solution parameters and fluid properties are defined in the parameter file [5]. The convergence criterion is 10E-06 and the solver is left to run until a converged solution is found [4], [6- 11].

### III.METHODOLOGY

A compressible air, with a Mach number of 2.95 flows over a double 15-degree angle wedge, as shown in Fig. 2.

#### A. Analytical solution

For the theoretical solution, oblique shock wave relations are used, and the free stream Mach number is 3.0 with a deflection angle of 15°. By applying the oblique wave relation,

$$M_2 = 2.2549$$

$$\beta = 32.2404^\circ$$

$$p_2/p_1 = 2.8215$$

$$T_2/T_1 = 1.3882$$

#### B. Numerical simulation

##### 1) Computational Domain

The computation domain was created using the ANSYS space claim, and the domain is shown in Fig. 6. All the data for the domain is in Table 1. Here we used deflection angle 15° which is half deflection angle; if geometry is mirrored, then it becomes 30° full deflection angle of the wedge.

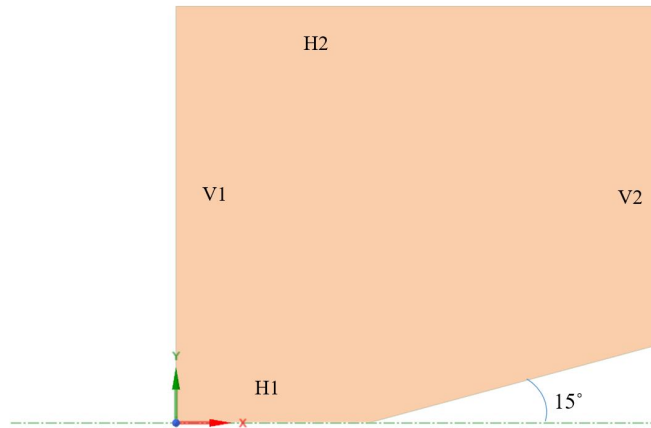


Fig. 6 Computational Domain of the Wedge

Table 1 Dimensions of the Domain

Notation	Length (m)
H1	0.6 m
V1	1.3 m
H2	1.5 m
V2	1.03 m

##### 2) Meshing

Meshing in Computational Fluid Dynamics (CFD) refers to the process of dividing a complex geometry into smaller, interconnected elements or cells. These elements collectively create a mesh, which forms a computational grid over the geometry. The mesh allows mathematical equations governing fluid flow to be solved numerically, enabling accurate simulation and analysis of fluid behaviour in various engineering scenarios. Proper meshing is crucial for obtaining reliable results in CFD simulations [12]. In this simulation, Face Meshing was used with the face. Then, for body Sizing, the element size was chosen 0.005m.

The number of nodes was calculated as 72048, and the number of elements was 71508. To capture the important flow parameter, the mesh needs to be refined near the region of interest [12,13].

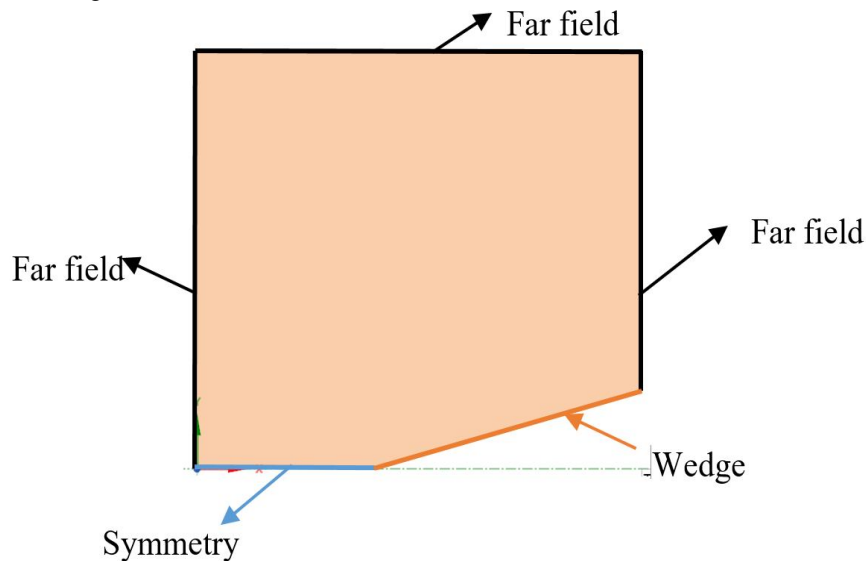


Fig. 7 Boundary Name

For simulation, the boundary conditions need to be specified at the various edges of the domain. In ANSYS Fluent, the "Pressure Far Field" boundary condition is used to simulate conditions at a region far away from the computational domain where the flow is approaching the boundary with a constant pressure. This boundary condition is often employed in external flow simulations where the exact pressure distribution is not known but the flow is assumed to be approaching the domain with a specific pressure value. The Pressure Far Field boundary condition helps simulate open boundary conditions effectively by specifying a reference pressure and inflow direction, allowing accurate representation of the inflow behaviour without the need for detailed information about the upstream conditions.

### 3) Solver Setup

The solver setup for flow over a wedge demands careful consideration of the specific characteristics of the problem, such as Mach number, angle of attack, and boundary conditions. A well-configured solver setup not only ensures accurate simulation results but also contributes to a deeper understanding of the complex flow phenomena associated with wedge geometries. In ANSYS Fluent, the first step is to define the general setting for the density- or pressure-based solver, as both models have their own characteristics that can influence the result of simulation. Pressure-based solvers are mostly used for incompressible and weak compressible flows, while density-based solvers are mostly used for compressible flows [14].

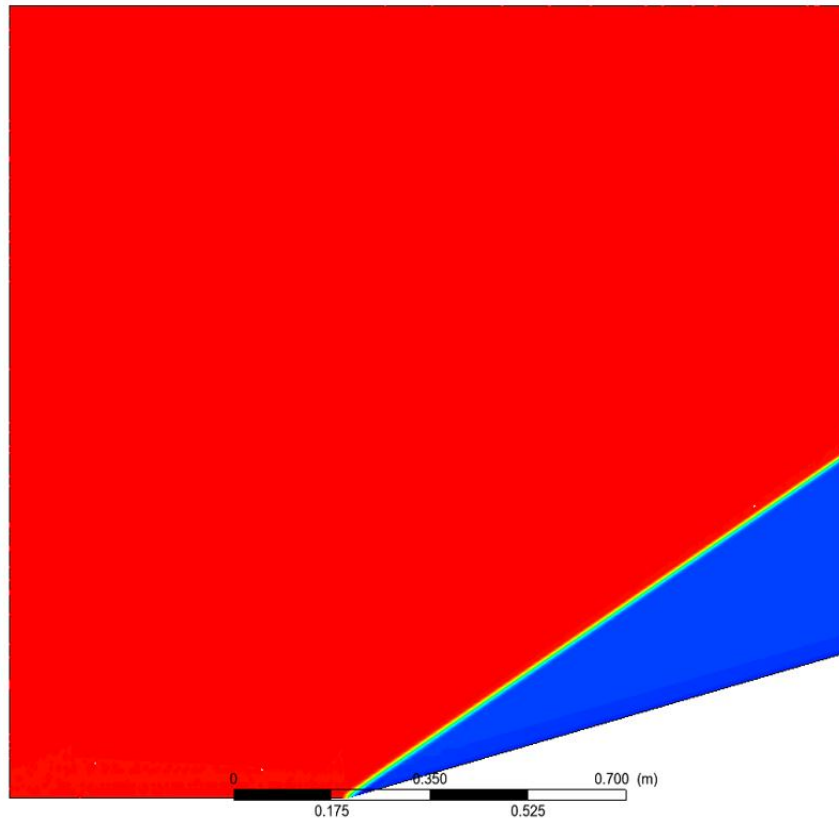
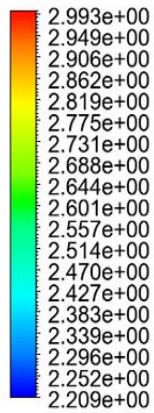
After that, a specific turbulence model needs to be chosen for a better and more accurate result. Here, the inviscid viscous model is used, and the air properties are changed to ideal gas because during the higher Mach number, the air behaves like ideal gas because the air molecules do not have time to interact with each other due to high kinetic energy, so for the higher Mach number, the air properties have to be changed to ideal gas [15].

The boundary condition of pressure far field is applied because the region is assumed to be free stream. In the solution method, under spatial discretization select the second-order upwind scheme as the first-order upwind scheme does not accurately capture sharp gradients or shock waves as it uses the value of the variable at the cell face to estimate the value of the variable at the cell centre, while the second-order upwind scheme uses a weighted average of the values of the variable at the cell face and the cell centre to estimate the value of the variable at the cell centre. This can lead to more accurate results for flows with sharp gradients [16].

In the initialization, standard initialization was applied and computed from the far field, and the number of iterations changed to 4000 for the calculation.

After that, the flow parameters such as Mach, pressure, and Temperature contours are visualised, as shown in Figs. 8, 9, and 10, respectively, and the results are analysed in the next section.

Mach Number  
Mach No



**Ansys**  
2023 R1  
STUDENT

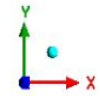
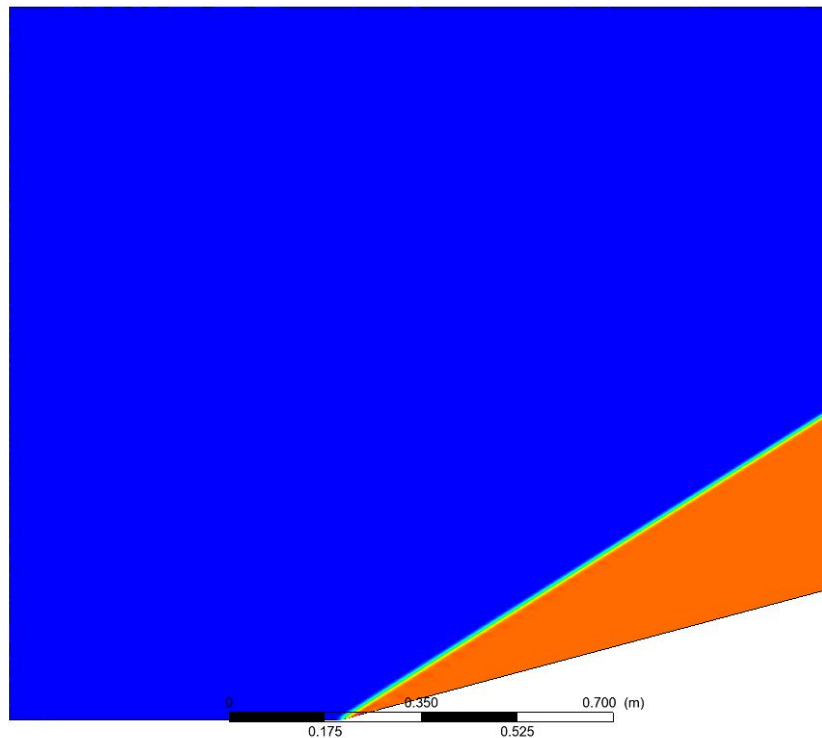
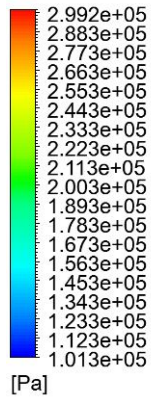


Fig. 8 Mach Contour

Pressure  
Pressure Contour



**Ansys**  
2023 R1  
STUDENT



Fig. 9 Pressure Contour

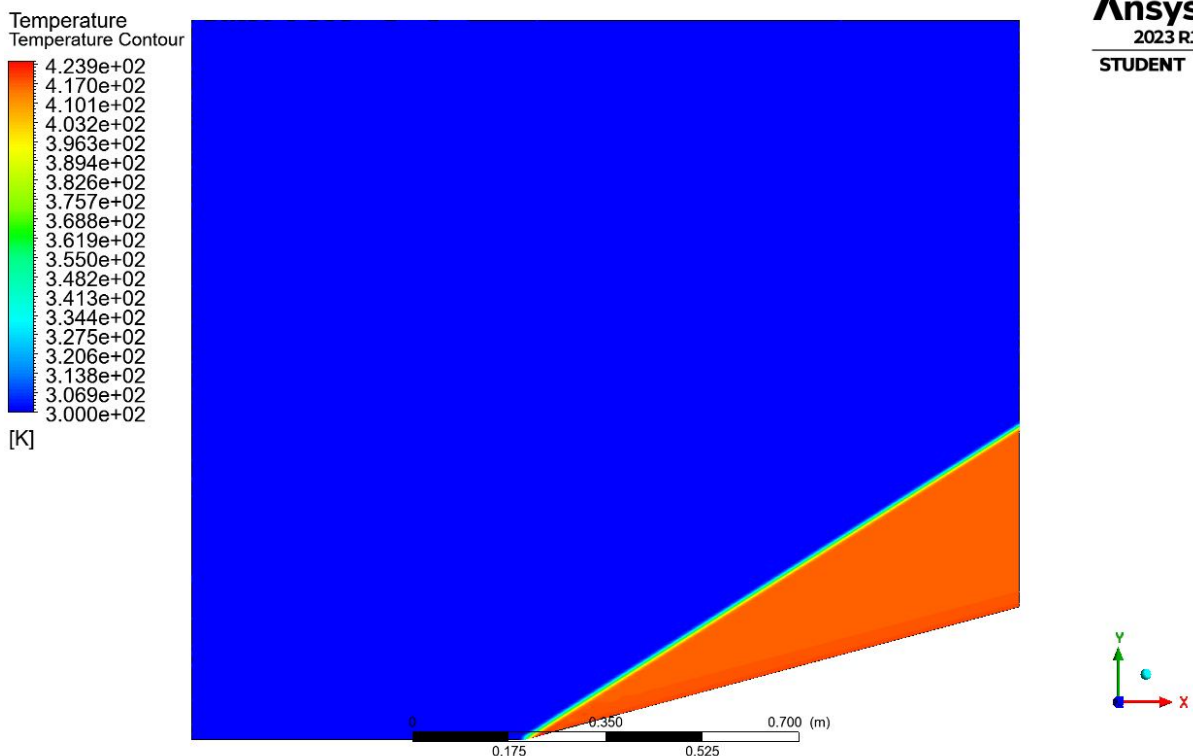


Fig. 10 Temperature Contour

#### IV. RESULTS AND DISCUSSION

The simulation was completed in 347 iterations, as the residual was given around  $10e^{-06}$ . After that, in the CFD post, the following parameter is analysed:

From the Mach contour, it is evident that behind the shock wave the Mach number is reduced considerably from 3 to 2.20, which is due to the shock wave. The shock wave reduces the velocity after the wave, which can be verified by the pressure contour, as air went through strong compression and the difference between before and after pressure is 101325 Pa and 300000 Pa, respectively. The temperature also changed drastically after the shock wave, as can be seen in Fig. 10. The free stream temperature was 300 K, and after compression it went up to 423 K.

The following charts show the flow parameter versus the length along the X-axis.

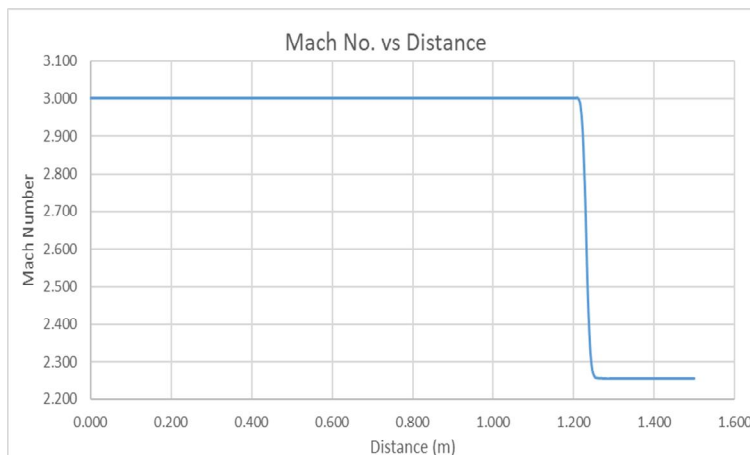


Fig. 11 Mach No vs. Distance



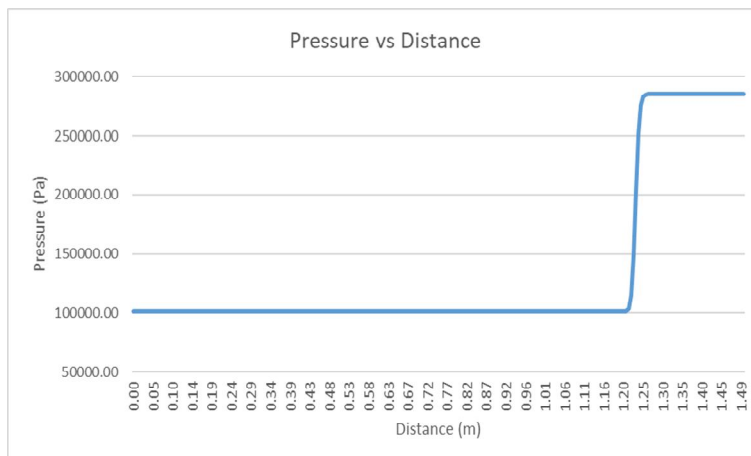


Fig. 12 Pressure vs. Distance

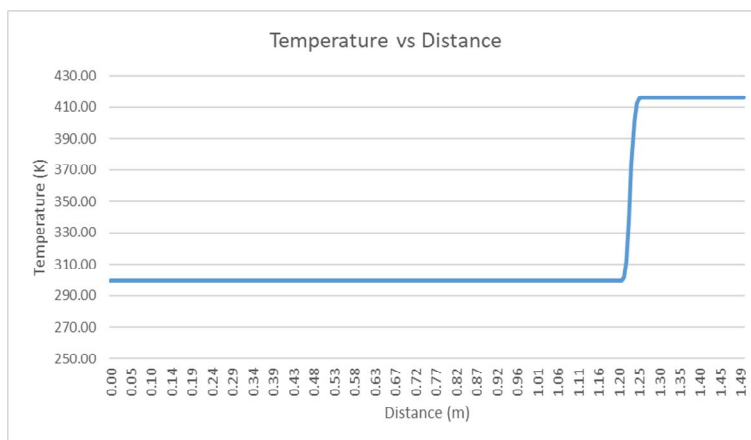


Fig. 13 Temperature vs. Distance

The chart of Mach number with respect to the X-axis shows the drastic decrement before and after the oblique shock wave; however, other properties such as Pressure and temperature are increased after the shock due to the strong compression.

The table below shows the percentage difference between the analytical results and the numerical simulation results.

Table 2 Comparison between Analytical and Fluent Results

Flow parameter	Analytical results	Fluent results	Percentage Difference
$M_2$	2.2549	2.2556	0.031%
$\beta$	32.2404°	32.2309°	0.029%
$p_2/p_1$	2.8215	2.8201	0.049%
$T_2/T_1$	1.3882	1.3873	0.064%

### V. CONCLUSIONS

In conclusion, this research project has produced a thorough examination of the complexities surrounding flow across a wedge, successfully merging the results of numerical simulation with analytical calculations. Using the computational power of ANSYS Fluent, the study meticulously simulated the complex dynamics of supersonic flow interactions with a Mach number of 3 and a 15° wedge-shaped structure. A wide range of flow parameters were subjected to meticulous examination and rigorous comparison with theoretically derived solutions sourced from oblique shock wave relationships. The striking agreement between the results of the numerical simulations and the analytical derivations highlights the effectiveness of both representational approaches for complex flow phenomena.

The modelling technique clearly showed how oblique shock waves during supersonic encounters with the wedge had a transformative effect on flow characteristics. The numerical calculations showed this: the post-shock Mach number showed a distinct decline to 2.25 from the initial free stream Mach number of 3, as shown by the numerical simulations. This sharp compression caused by the oblique shock phenomenon is responsible for the simultaneous rise in temperature and pressure. This study supports the ability of numerical simulation to render precise forecasts while expertly capturing complex flow discontinuities. The comprehensive comparison of many parameters in Table 2's tabular portrayal of these results strengthens the validity of both techniques. This thorough comparison study demonstrates the reliability of numerical simulation as a tool for understanding flow dynamics, especially the complex behaviour brought on by oblique shock waves.

In conclusion, the symbiotic integration of numerical simulation and analytical computation, as highlighted in this study, confirms their combined effectiveness in explaining the complex details of flow through a wedge. The knowledge gained here helps us better understand these flow phenomena and paves the way for future research into similar phenomena in a variety of engineering fields.

## REFERENCES

- [1] J. D. Anderson, "Inviscid, Compressible Flow," in *Fundamentals of aerodynamics*, New York, NY: McGraw-Hill Education, 2017, pp. 587–630
- [2] A. H. Shapiro, "Oblique Shocks," in *The dynamics and thermodynamics of compressible fluid flow*, New York: Ronald Press, 1958
- [3] S. Bender and O. A. Sadik, "Direct electrochemical immunosensor for polychlorinated biphenyls," *Environmental Science & Technology*, vol. 32, no. 6, pp. 788–797, 1998. doi:10.1021/es9705654
- [4] K. Alhussan, "Computational analysis of high speed flow over a double-wedge for air as working fluid," *Volume 2: Fora*, 2005. doi:10.1115/fedsm2005-77441
- [5] M. Rahman and C. A. Brebbia, "Experiment versus Simulation," in *Advances in fluid mechanics VII*, Ashurst, Southampton: WIT, 2008, pp. 131–210
- [6] K. Alhussan, W. J. Hong, and C. Garris, "Non-steady pressure-exchange ejector," *Volume 1: Fora, Parts A and B*, Jul. 2002. doi:10.1115/fedsm2002-31307
- [7] K. Alhussan and C. Garris, "Non-steady three-dimensional flow field analysis in supersonic flow induction," *Volume 1: Fora, Parts A and B*, Jul. 2002. doi:10.1115/fedsm2002-31088
- [8] K. Alhussan and C. Garris, "Computational analysis of flow inside a diffuser of three-dimensional supersonic non-steady ejectors," *Fluids Engineering*, vol. 1, no. 3, pp. 504–512, Jul. 2005. doi:10.1115/imece2005-80843
- [9] K. Alhussan and C. Garris, "Study the effect of changing inlet area ratio of a supersonic pressure-exchange ejector," *43rd AIAA Aerospace Sciences Meeting and Exhibit*, Jan. 2005. doi:10.2514/6.2005-519
- [10] K. Alhussan, "Computational analysis of high speed flow over a conical surface with changing the angle of attack," *Procedia Engineering*, vol. 61, pp. 48–51, Sep. 2013. doi:10.1016/j.proeng.2013.07.091
- [11] K. Alhussan and C. Garris, "Effect of changing throat diameter ratio on a steam supersonic pressure exchange ejector," *Modern Physics Letters B*, vol. 19, no. 28 & 29, pp. 1715–1718, Jun. 2005. doi:10.1142/s0217984905010293
- [12] A. Guardo, M. Coussirat, M. A. Larrayoz, F. Recasens, and E. Egusquiza, "Influence of the turbulence model in CFD modeling of wall-to-fluid heat transfer in packed beds," *Chemical Engineering Science*, vol. 60, no. 6, pp. 1733–1742, Oct. 2005. doi:10.1016/j.ces.2004.10.034
- [13] C. R. Prajapati, A. P. Donga, P. R. Babariya, and A. D. Patel, "Comparative Analysis OF Turbulence Models FOR Simulating Flow Over a Flat Plate.," *International Journal of Engineering Applied Sciences and Technology*, 2023, vol. 8, no. 01, pp. 278–283, May 2023.
- [14] L. Mangani, W. Sanz, and M. Darwish, "Comparing the performance and accuracy of a pressure-based and a density-based coupled solver," *16th International Symposium on Transport Phenomena and Dynamics of Rotating Machinery*, Apr. 2016. hal-01894391
- [15] R. D. Zucker and O. Biblaraz, "Moving and Oblique Shocks," in *Fundamentals of Gas Dynamics*, 2nd edition, Hoboken, New Jersey: John Wiley & Sons, 2002, pp. 179–189
- [16] J. D. Anderson, *Computational Fluid Dynamics: The Basics with Applications*. New York, NY: McGraw-Hill, 2010.
- [17] *Supersonic Flow Over a Wedge Analysis - Ansys Innovation courses*, [https://courses.ansys.com/wp-content/uploads/2021/12/Autoconstraints-2-300x225\\_New-5.png](https://courses.ansys.com/wp-content/uploads/2021/12/Autoconstraints-2-300x225_New-5.png) (accessed Aug. 15, 2023).



10.22214/IJRASET



45.98



IMPACT FACTOR:  
7.129



IMPACT FACTOR:  
7.429



# INTERNATIONAL JOURNAL FOR RESEARCH

IN APPLIED SCIENCE & ENGINEERING TECHNOLOGY

Call : 08813907089  (24\*7 Support on Whatsapp)